



# Evaluation of Slurry Erosive Wear Performance of Plasma-Sprayed Flyash-TiO<sub>2</sub> Composite Coatings

R. Keshavamurthy<sup>1</sup> · B. E. Naveena<sup>2</sup> · C. S. Ramesh<sup>3</sup> · M. R. Haseebuddin<sup>1</sup>

Received: 14 January 2021 / Revised: 18 April 2021 / Accepted: 22 April 2021 / Published online: 13 May 2021  
© The Author(s), under exclusive licence to Springer Nature Switzerland AG 2021

## Abstract

The present research is intended at the development of plasma-sprayed coatings of Flyash-TiO<sub>2</sub> on the Al-6061 substrate. The coatings were developed under optimum process conditions and subjected to evaluate the slurry erosive wear characteristics in 3.5% NaCl solution with varying levels of operating factors such as slurry concentration, slurry rotation speed, impinging particle size, and test duration. Under identical test conditions, the developed coatings demonstrate a 52% enhancement in slurry erosive wear resistance compared to the uncoated Al-6061 alloy. The Scanning Electron Microscopy (SEM) and Confocal Microscopy (CM) were used to examine the eroded surfaces of coated and uncoated specimens under varying test conditions. It is identified that severe plastic flow is observed in uncoated alloy, and curtailed damage of surfaces in the case of coated substrates confirms superior slurry erosion resistance in coatings compared to uncoated ones. Six-fold enhancements in the surface hardness and corrosion resistance are the main reasons for improved slurry erosive wear performance of coatings compared to alloy.

**Keywords** Plasma spray · Flyash · Titania · Al-6061 · Slurry erosive wear

## 1 Introduction

A phenomenon involving degradation of the target surface by the impingement of entrapped abrasive particles in a liquid medium is defined as slurry erosive wear. This process requires strain rates of high value leading to surface degradation by way of loss of material. Service life and material durability are factors affecting the erosion phenomenon. This in turn leads to premature failures of engineering components (hydroelectric power plants, fluid machinery in mining, marine, agricultural sector, and petroleum industry), resulting in expensive breakdowns and huge productivity losses [1–3]. These issues can be overcome either by using high-cost erosion-resistant alloys or enhancing the wear

resistance of the existing metals by adopting effective surface modification techniques.

The numerous industrial methods of surface modifications specially used are heat treatment, thermal spraying, hot dipping, chemical and physical vapor depositions, electroless plating, electro-plating, and weld overlaying. In these methods, thermal spray techniques gain an extensive reputation to develop products that will meet all surface phenomena' desires and make certain competitiveness in the domain [4, 5].

The Atmospheric Plasma Spraying (APS) process is one of the best choices among the available thermal spray techniques to coat metal, ceramics, and cermets on the surface of new components or rebuild on worn parts for various applications. Hence, plasma spraying emerged as the most versatile and adaptable method to offer a wide range of quality/cost and has been extensively accepted in areas experiencing extensive surface degradation and requiring frequent replacement [6, 7].

Plasma-sprayed ceramic coatings are most often used in industrial components where anti-wear and anti-corrosion characteristics are associated with the concerned applications. In many manufacturing sectors, oxide ceramics, particularly Cr<sub>2</sub>O<sub>3</sub>, Al<sub>2</sub>O<sub>3</sub>, TiO<sub>2</sub>, and ZrO<sub>2</sub>, are mainly used for

✉ R. Keshavamurthy  
keshavamurthy.r@gmail.com

<sup>1</sup> Department of Mechanical Engineering, Dayananda Sagar College of Engineering, Bangalore 560078, India

<sup>2</sup> Department of Automobile Engineering, Dayananda Sagar College of Engineering, Bangalore, Karnataka 560 078, India

<sup>3</sup> Department of Mechanical Engineering and Dean, Research & Innovation, Presidency University, Bangalore, India

**Table 1** Plasma spray conditions

Spray factors	Value
Density of current	470 amps
Stand-off distance	65 mm
Feed rate of powder	55 g/min

erosion-resistant applications to adopt plasma spray techniques effectively. Titanium dioxide ( $\text{TiO}_2$ ) is an established and widely used oxide material for thermally sprayed coating solutions because of its relatively low melting point and thermal conductivity. The interest in it has escalated in last few years because of its specific multifunctional properties and the variety of its current and possible applications [8–11]. Ramesh et al. [12] investigated the slurry erosive property of plasma-coated  $\text{TiO}_2$ -30 wt% Inconel-718 with NiCr as a bond coat on the copper substrate. They have observed that a developed coating of 200  $\mu\text{m}$  exhibited superior slurry erosive resistance than coatings with 100  $\mu\text{m}$  thickness. Chinakurli Suryanarayana et al. [13] made a similar observation that slurry erosive wear resistance of developed  $\text{TiO}_2$  with 30 wt% Inconel-718 plasma coating significantly combated slurry wear rate than the bare Al-6061 substrate under all test conditions. Zaki Ahmad et al. [14] have concluded that  $\text{TiO}_2$  plasma coatings offer superior resistance to erosion-corrosion in a 3.5 wt% NaCl-aerated environment. Ville Matikainen et al. [15] have made a study on the abrasion, erosion, and cavitation erosion wear behavior of plasma-sprayed  $\text{Al}_2\text{O}_3$ -based coatings. Results indicated that plasma sprayed from agglomerated and sintered  $\text{Al}_2\text{O}_3$ - $\text{TiO}_2$  coatings impressively combated erosive wear compared with unalloyed  $\text{Al}_2\text{O}_3$  coatings.

The cost of manufacturing plasma-spray-grade powders makes the process very expensive and limits the application possibilities. In the last two decades, many researchers have studied plasma coatings for various engineering applications. Nevertheless, very few researchers have reported on utilizing low-cost feedstock materials for plasma spray applications.

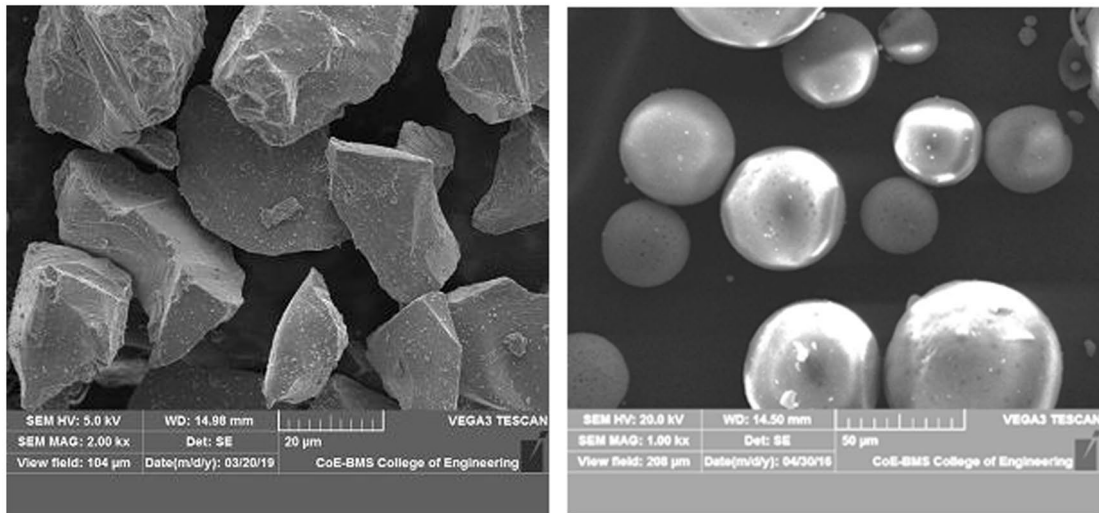
Flyash is an industrial waste by-product and inexpensive material, available abundantly from various thermal power plants. If not suitably disposed and recycled, it can be a primary source and cause of pollution and interrupt ecological stability. This will pose serious health hazards to human beings. Therefore, there's essential to reutilize flyash in manufacturing and construction applications using appropriate methods. By utilizing flyash for thermal spray applications, it could be effectively transformed into green material. According to a few researchers, flyash as a feedstock material has exhibited great potential for developing plasma coatings on various substrates, as it contains oxides of aluminum, silicon, iron, and calcium, which will enhance its performance to overcome high temperatures, corrosion,

**Fig. 1** Photograph of slurry erosion wear tester

erosion, and wear [16, 17]. Mishra et al. [18] have successfully deposited flyash coating on the metal substrate using plasma technology and stated that flyash has excellent potential as a feedstock material for developing a plasma spray coating. Buta Singh Sidhu et al. [19] evaluated the plasma method's flyash coatings' corrosion and wear behavior. They have concluded that the presence of  $\text{SiO}_2$  and  $\text{Al}_2\text{O}_3$  in flyash enhanced the corrosion and wear resistance of coated substrate considerably. Yılmaz et al. [20] have studied the potential use of flyash (with and without different composition of Al powder) as a feedstock material for plasma spray coatings and reported that flyash is a cost-effective coating material and can be used for various engineering applications. Also, they have noticed that the addition of Al powder enhances the adhesive strength of coatings.

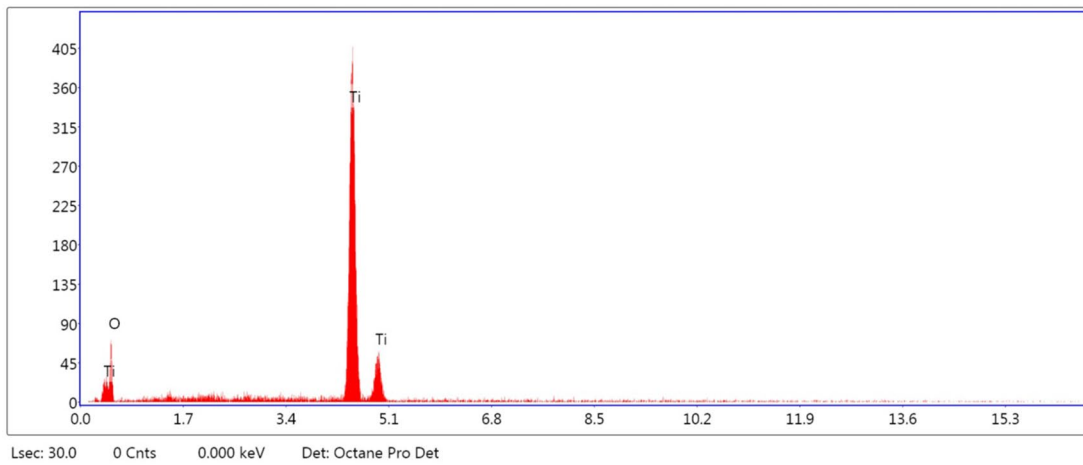
Thus, combining flyash- $\text{TiO}_2$  as composite feedstock powders, the ensuing thermal spray coatings will benefit the individual properties like higher modulus, hardness, wear, and corrosion resistance, thereby enhancing the cost-effectiveness in plasma spray technique with value addition using potential low-cost composite feedstock materials.

Considering the above discussions, the present research focuses on developing plasma-sprayed Flyash- $\text{TiO}_2$  composite coatings on the Al-6061 alloy substrate. Further, the coatings produced under optimum process conditions are subjected to evaluate the slurry erosive wear characteristics under varying operating factors such as the slurry concentration, slurry rotation speed, impinging particle size, and test duration.

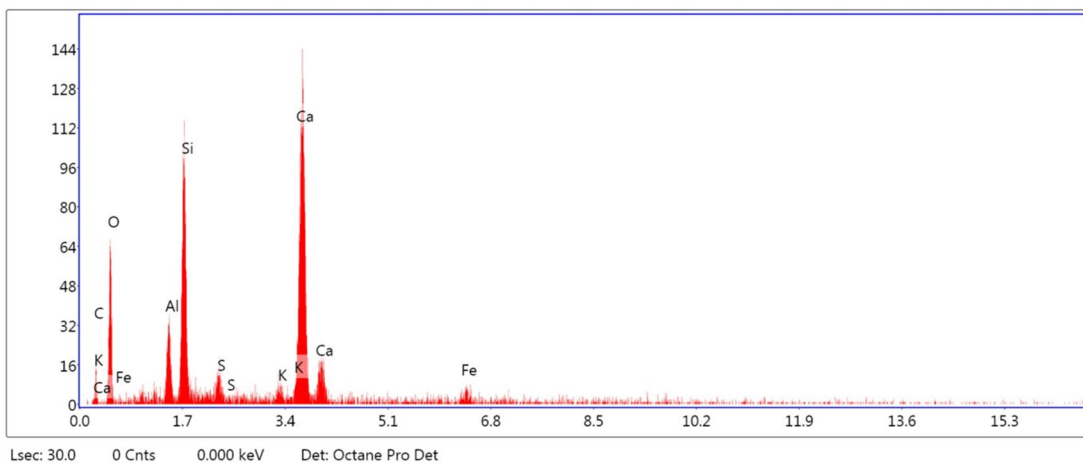


(a) SEM of TiO<sub>2</sub> particles

(b) SEM of Flyash particles



(c) EDAX Photograph of TiO<sub>2</sub> Powder



(d) EDAX Photograph of Flyash Powder

**Fig. 2** a SEM of TiO<sub>2</sub> particles. b SEM of Flyash particles. c EDAX photograph of TiO<sub>2</sub> powder. d EDAX Photograph of Flyash Powder

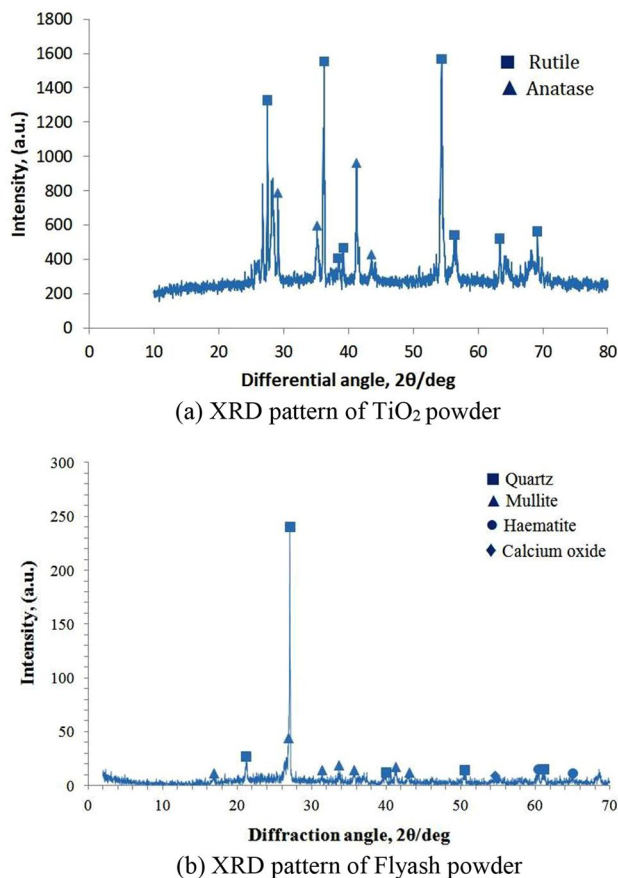


**Fig. 3** **a** XRD pattern of TiO<sub>2</sub> powder. **b** XRD pattern of Flyash powder

## 2 Materials and Methods

### 2.1 Materials

Among the several high-strength aluminum alloys, the 6000 series, which is alloyed with magnesium and silicon, has become the most appealing material in engineering applications where lightweight with higher specific strength and corrosion resistance is essential. As Aluminum 6061 alloy had a wide range of applications in marine, automotive, and aerospace industries, it was designated as substrate. Commercially available Al-6061 alloy plates were cut and grounded to 100 mm × 100 mm × 10 mm dimensions. Commercial grade Titanium dioxide powder with particle size range 20–40 μm and flyash (Class-F) powder with particle size range 20–60 μm were used as feedstock materials. These powders were premixed in equal weight ratios to coat on Aluminum 6061 substrate. A combination of these feedstock powders were blended using a planetary mixer

for 30 min at 20 rpm to ensure uniform mixing before being thermally deposited by APS.

### 2.2 Thermal Spraying

The substrate plates were made ready for coating deposition by grit blasting to maintain a uniform surface roughness (Ra) of 1.5 μm for proper bonding and thoroughly cleaned in acetone to remove all dust particles from the surface. Subsequently, a plasma-sprayed 50 μm metallic bond is deposited using NiCr alloy onto the substrate to reduce the thermal expansion coefficients mismatch between ceramic top coats metal substrate. After this, the top-coat of 100-μm-thick Flyash-TiO<sub>2</sub> composite coating was deposited by Sulzer-Metco 3 MB Plasma torch adopting optimized spray parameters. Optimization was performed using Taguchi's Design of Experiments (DoE) method as per L<sub>9</sub> orthogonal arrays for attaining higher surface hardness and lower porosity. Table 1 presents the optimum process condition implemented in this study. Further, Argon and hydrogen were used as carrier gases with flow rates of 80–90 lpm and 20–25 lpm, respectively. Furthermore, the voltage of 60 V was kept constant throughout the experiments.

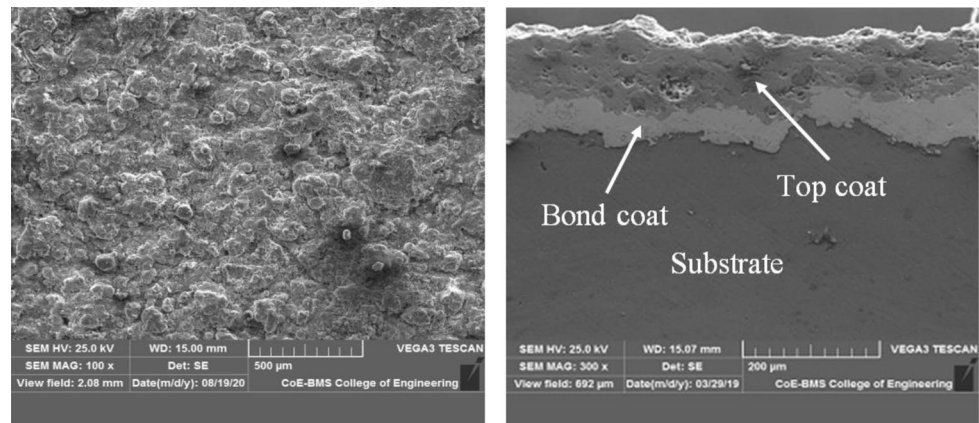
### 2.3 Characterization

Microstructural studies of synthesized coatings were carried out on polished samples using the MEIJI metallurgical optical microscope. SEM and EDAX studies were carried out (VEGA3 TESCAN), at BMS college of Engineering Bengaluru, India, for the feedstock powders and coatings to analyze the morphology, elemental composition surface topography, and wear mechanisms. X-ray diffraction analysis of feedstock powders and developed coatings were captured using Philips X'Pert Pro X-ray diffractometer. Confocal Microscopy (CM) studies were performed using Olympus LEXT 4000 microscope to examine eroded surface morphology. The Micro-hardness test was performed on metallographically polished cross-sections of coatings with 5 N load and 10 s dwell time using MH-3C, Vickers' micro-hardness tester (Make: Everone Enterprises, Hong Kong).

Five different coating locations were indented for hardness measurement, and the average value of all readings was considered the final hardness of specimens. A slurry erosion test was conducted on samples of size 75 × 25 × 10 mm using a slurry erosion tester (Model: SW2019, Make: Micro-matic Technologies, Bengaluru, India). Photograph of slurry erosion wear tester used in this study is shown in Fig. 1. The apparatus consists of an electric motor with a speed controller to regulate the four sets of spindles' speed by a belt drive. The samples are fixed on each of the spindles and submerged within the stainless-steel slurry cups having the slurry combination of 35 g of NaCl with the required

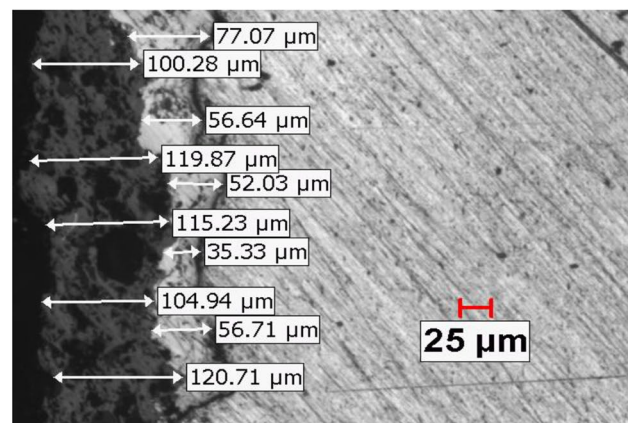


**Fig. 4** **a** SEM of Flyash-TiO<sub>2</sub>-coated specimen. **b** SEM of cross-sectional view of Flyash-TiO<sub>2</sub> coatings. **c** Optical images of Flyash-TiO<sub>2</sub> coating



(a) SEM of Flyash-TiO<sub>2</sub> coated specimen

(b) SEM of cross-sectional view of Flyash-TiO<sub>2</sub> coatings



(c) Optical images of Flyash-TiO<sub>2</sub> coating

quantity of silica sand in one liter of distilled water. Before the test, the specimens were cleaned thoroughly, dried, and weighed. The influence of variation in levels of factors like slurry speed (500, 1000, and 1500 rpm), the concentration of slurry (10, 20, and 30 g/l), the sand particle size (210, 300, and 425 μm), and test period (3.6 and 9 h) was studied [2, 3, 21]. A precision electronic weighing scale was used to record the cumulative weight loss of dried and cleaned specimens.

### 3 Results and Discussion

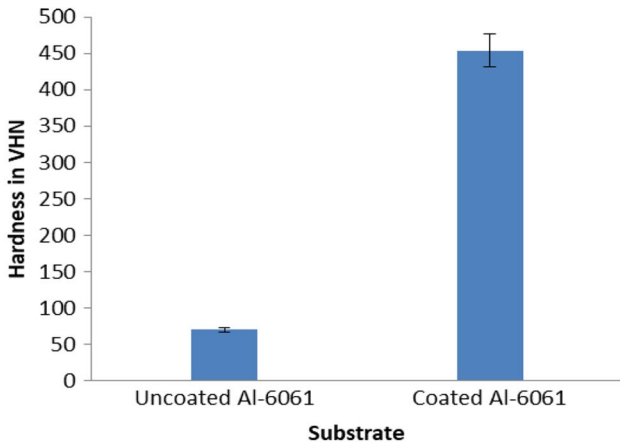
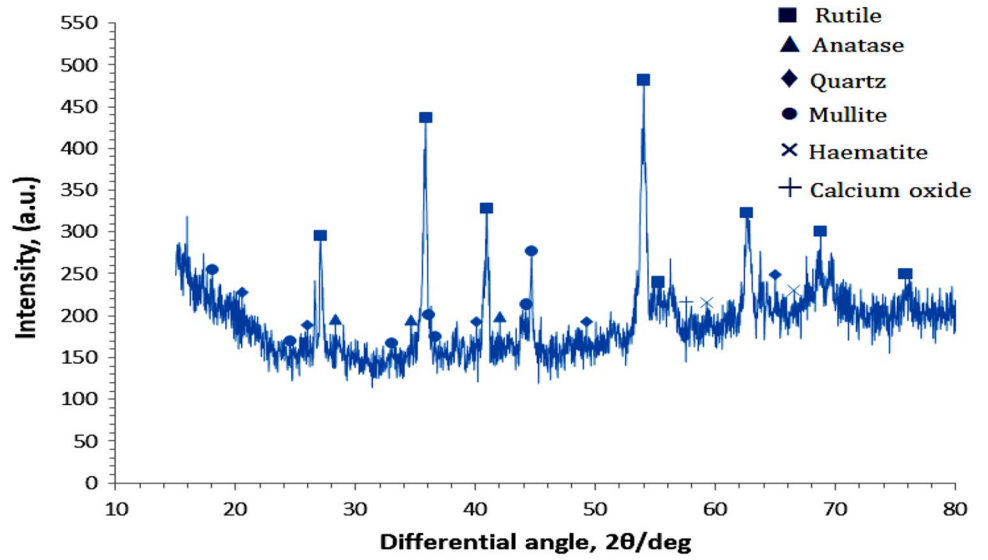
#### 3.1 Analysis of Feedstock Powders

Figure 2a and b illustrate the SEM of the feedstock powders used in the current study, namely, Titania and Flyash. Morphological studies indicate that the TiO<sub>2</sub> particles have an angular shape, with 20–40 μm range of particle size. Flyash powders have an average size of particle 20–60 μm with a spherical shape in morphology. Energy Dispersive

Spectroscopy is also performed to identify the elemental composition of feedstock powders. EDAX patterns of TiO<sub>2</sub> powder in Fig. 2c reveal the presence of oxygen with weight 44.43% and titanium with a weight 55.57%. Figure 2d confirms quartz, mullite, hematite, and calcium oxide (cubic structure) in the flyash feedstock powders. These would implicate improved wear, erosion, and corrosion resistance properties of developed composite coatings [7].

X-ray diffraction studies were performed to identify the atomic and molecular structure of feedstock powders. XRD patterns of TiO<sub>2</sub> feedstock powder, as seen in Fig. 3a. This exhibits the firm diffraction peaks at 27°, 36°, and 55° confirming that the rutile phase is dominating when compared with the anatase phase. The rutile phase is tetragonal and possesses a higher hardness value when compared with the anatase phase [21]. XRD of flyash shown in Fig. 3b reconfirms the presence of oxides of quartz, mullite, hematite, and calcium in the flyash feedstock powders.

**Fig. 5** XRD of Flyash-TiO<sub>2</sub>-coated specimen

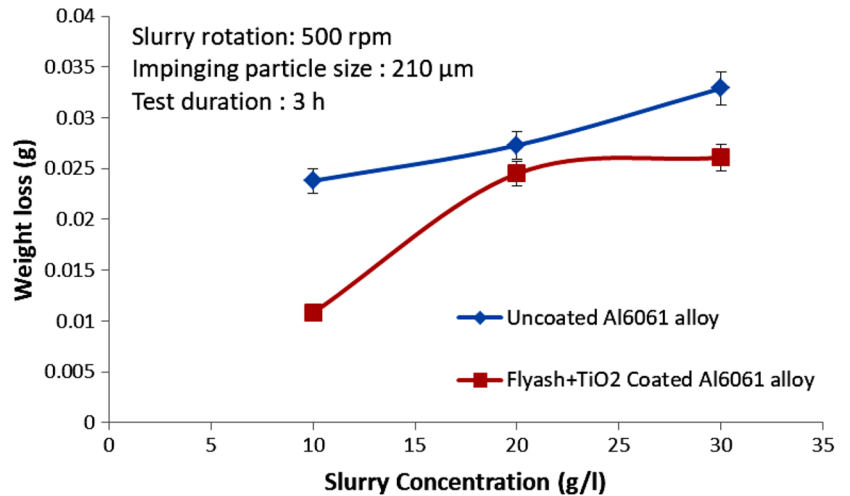


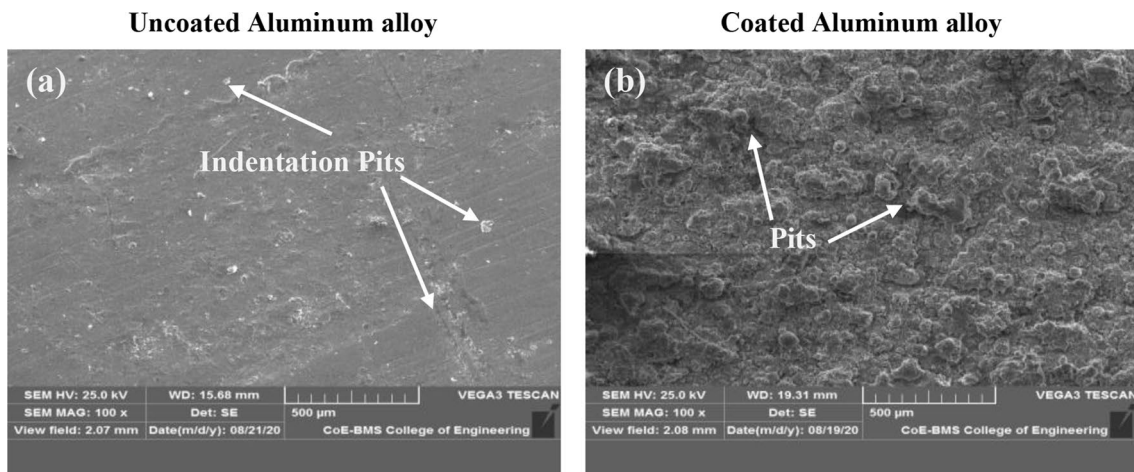
**3.2 Microstructure**

The SEM and optical micrographs of the cross-sectional view of developed Flyash-TiO<sub>2</sub> composite coatings on the Al-6061 substrate are shown in Fig. 4a-c. There is a homogeneous and intense deposition of splats without any visible cracks or defects. The bond between the coating and the substrate is good, and the average thickness of the developed composite coatings is 150 μm, including 50 μm of NiCr bond coat, as evidenced by the cross-sectional surface microphotographs. Figure 5 shows the XRD pattern of flyash-TiO<sub>2</sub> coatings and confirms all major alloying elements of the top-coat.

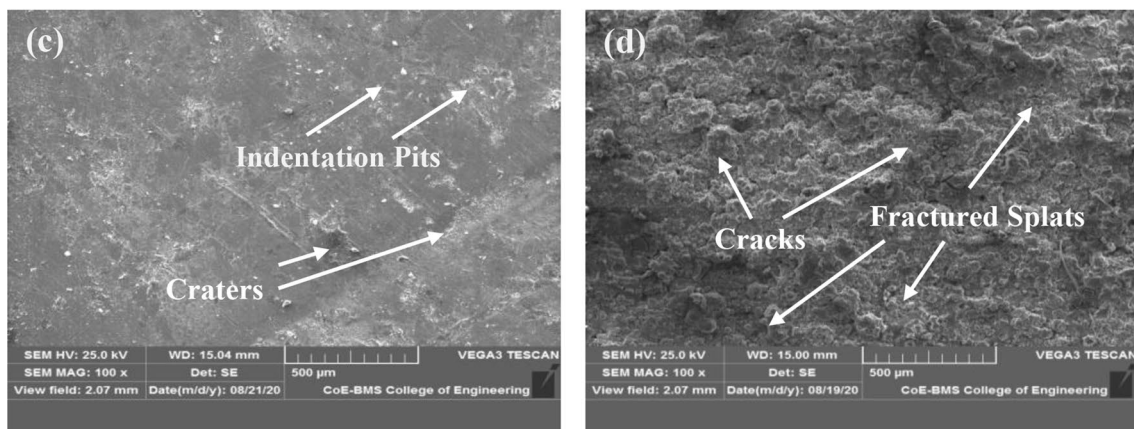
**Fig. 6** Graphical representation of micro-hardness

**Fig. 7** Weight loss at different concentration of slurry

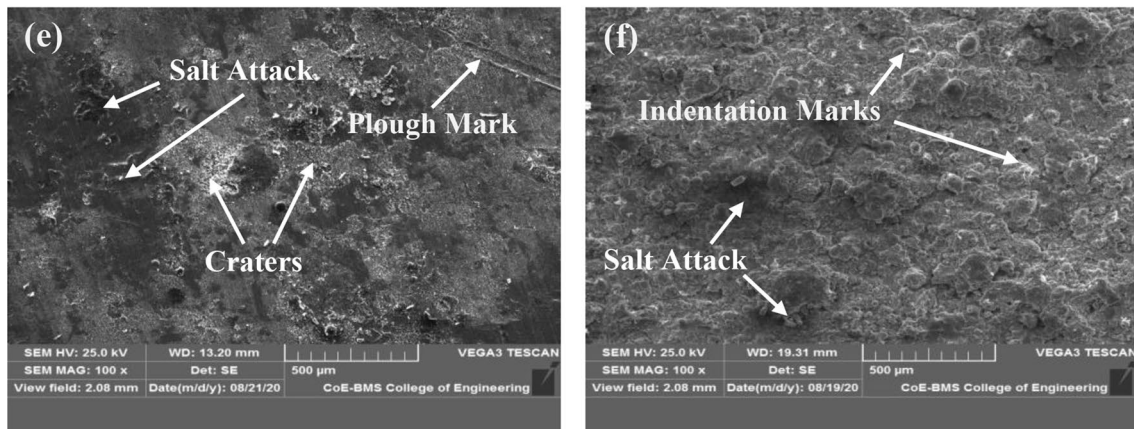




(a) & (b) uncoated and coated substrate at 10 g/l



(c) & (d) uncoated and coated substrate at 20 g/l



(e) & (f) uncoated and coated substrate at 30 g/l

**Fig. 8** a–f SEM of eroded surfaces at different concentration of slurry. **a** and **b** Uncoated and coated substrate at 10 g/l. **c** and **d** Uncoated and coated substrate at 20 g/l. **e** and **f** Uncoated and coated substrate at 30 g/l

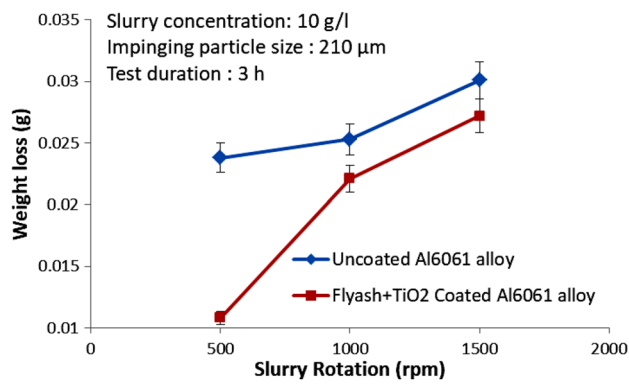


**Fig. 9** Weight loss at different slurry rotation speed

### 3.3 Micro-Hardness

Figure 6 shows the variation of micro-hardness (HV) for uncoated and coated Al-6061 substrate with 5 N applied for 10 s reside times. It is noticed that synthesized coating shows a tremendous enhancement in micro-hardness. An average micro-hardness of 454 HV<sub>5N</sub> was observed for developed Flyash-TiO<sub>2</sub> coatings, which is nearly 6.5-fold higher than the uncoated Al-6061 substrate (70 HV<sub>5N</sub>). The improved hardness of coatings can be accredited to the uniform deposition with lower porosity levels and higher hardness of feedstock. This would positively contribute to the inclusive wear, erosion, and corrosion resistance of coatings compared to the bare substrate [22].

### 3.4 Slurry Erosion Test

#### 3.4.1 Influence of Slurry Concentration

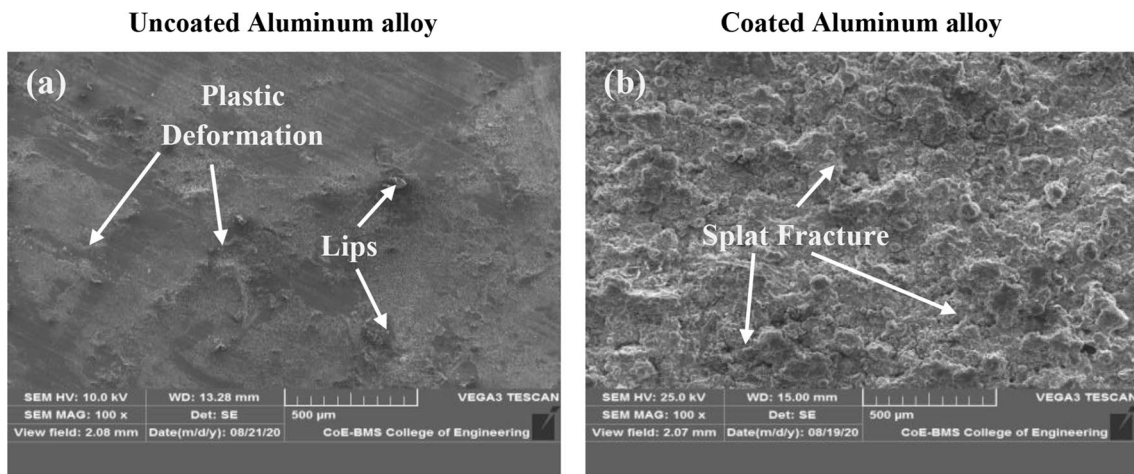
Figure 7 illustrates the weight loss of both uncoated and Flyash-TiO<sub>2</sub>-coated Al-6061 substrate for the slurry concentrations of 10, 20, and 30 g/l with the constant slurry speed of 500 rpm, 3 h duration, and 210 μm impinging particle size. It is noticed that an increase in the concentration of slurry has caused more significant weight loss. This is due to the increased probability of an attack on the samples as slurry concentration increases and leads to excessive erosive

wear. SEM micrographs (Fig. 8a–f) reveal massive pitting holes all across the substrate's surface, indicating a clear sign for the uncoated substrate's susceptibility to the corrosive NaCl solution. Additionally, many surface cracks with craters have been noticed, mainly resulting from slurry particles' impingement. However, it exhibits shallow susceptibility for coated substrate compared to the uncoated Al-6061 substrate at any specified slurry concentration. It can be concluded that the increased concentration of solid particles in the slurry increases the severity of synergic erosion-corrosion, and indentation by impinging particles turns into a significant factor leading to the increased surface deterioration [3, 13, 23].

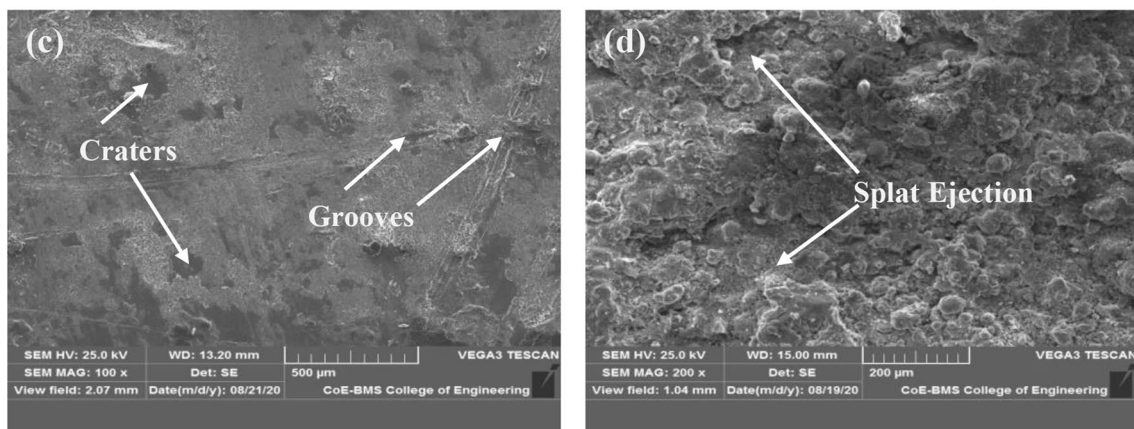
#### 3.4.2 Influence of Slurry Rotation Speed

The weight loss of uncoated and Flyash-TiO<sub>2</sub>-coated substrates for varying slurry rotation speeds of 500, 1000, and 1500 rpm with a fixed time, the slurry concentration, and particle size are shown in the Fig. 9. It is illustrated that with an escalation in slurry speed, the slurry erosion rates of test specimens' increased. The trend observed is in line with other researchers [2, 12, 21]. An extreme material loss is captured at a maximum rotation speed of 1500 rpm compared to lower speeds. This is because an increase in slurry speed will enhance the kinetic energy of erodent and the rate of slurry interaction on the target surfaces. This more considerable kinetic energy gets transformed into both heat energy and plastic deformation; consequently, more weight loss occurred with localized attacks at several areas on the target surfaces [24]. It can be noticed with evidence of SEM morphology (Fig. 10a–f) of uncoated and coated samples after a slurry erosion test. The extent of damage increased as slurry speed increases due to the augmentation in plastic deformation and heat generation, causing grooves, lips, and crater shapes on both the coated and bare substrates. Here, the composite of Flyash-TiO<sub>2</sub> coating exhibited the least deterioration because of its higher density and surface hardness, which makes it more resistant to slurry erosive wear.

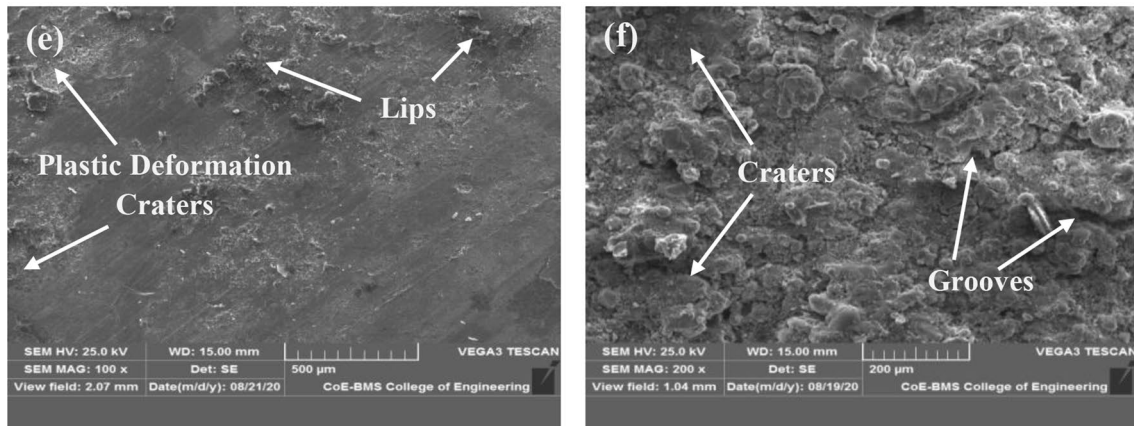




(a) &amp; (b) uncoated and coated substrate at 500 rpm



(c) &amp; (d) uncoated and coated substrate at 1000 rpm



(e) &amp; (f) uncoated and coated substrate at 1500 rpm

**Fig. 10** a–f SEM of eroded surfaces at the different slurry rotation speed. **a** and **b** Uncoated and coated substrate at 500 rpm. **c** and **d** Uncoated and coated substrate at 1000 rpm. **e** and **f** Uncoated and coated substrate at 1500 rpm

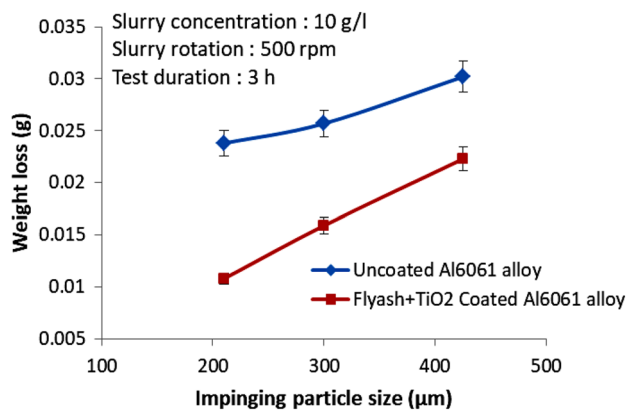


**Fig. 11** Weight loss at different impinging particle size

### 3.4.3 Influence of Impinging Particle Size

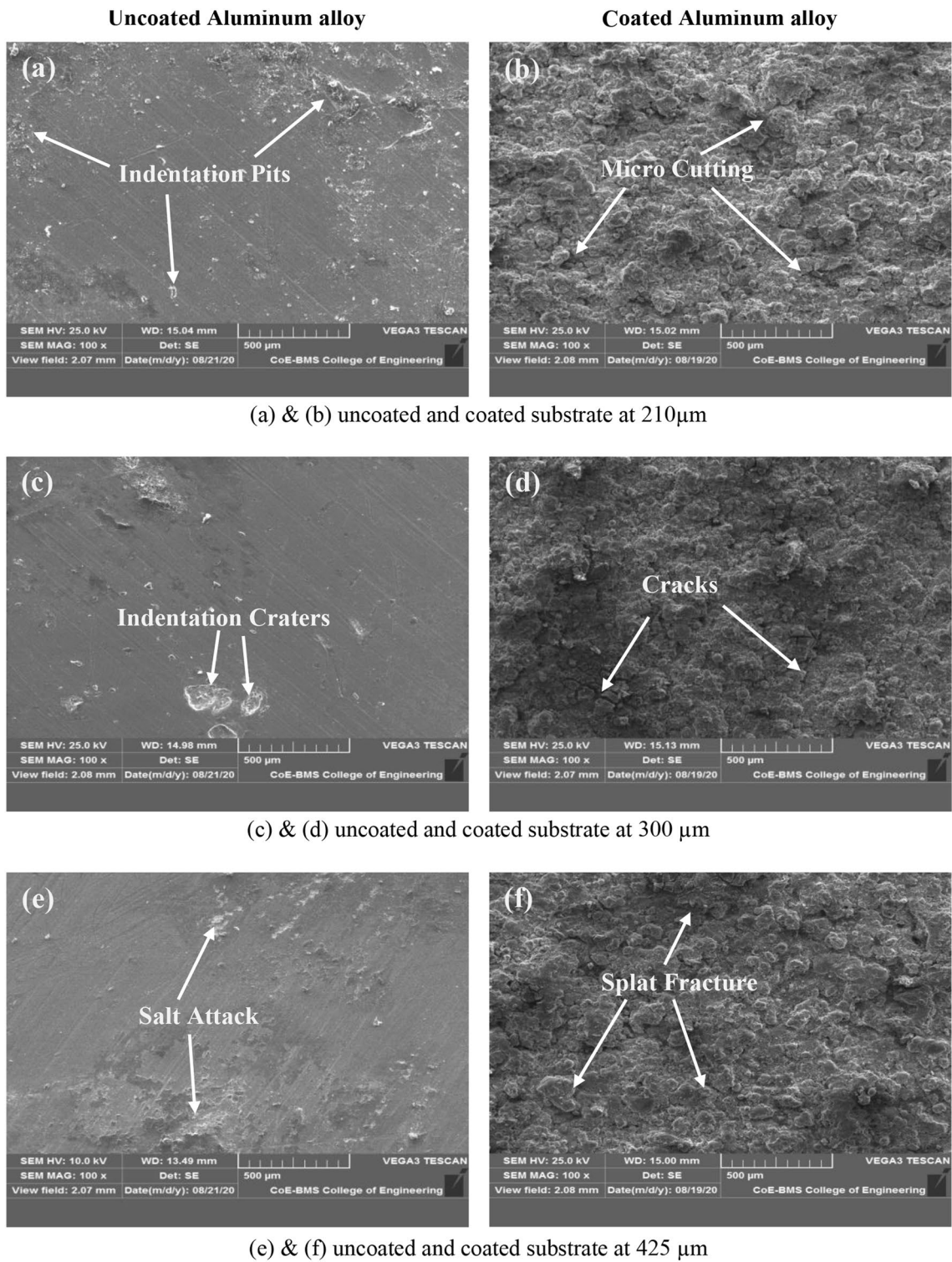
Figure 11 indicates the weight loss of uncoated and coated Al-6061 substrate with an increase in the impinging particle size of 210, 300, and 425 μm with constant test time and slurry speed and concentration. It is observed that there is an increasing trend of weight loss with increased particle sizes. This is articulated to the more massive particle's ability to directly apply their mass and energy to the target material's surface with very little interaction. Also, an upsurge of impinging particle size in the slurry would result in an increased surface area of the particle with other cutting edges, leading to wear loss. Small-sized impinging particles have lower impact stress due to lower particle energy, leading to minimized weight loss [21, 24]. Figure 12a–f shows that the uncoated Al-6061 alloy was eroded more severely than a coated substrate due to lower hardness and corrosion resistance compared to Flyash-TiO<sub>2</sub>-coated substrate.

Further, many indentation pits, grooves, and craters have been observed on eroded bare substrates, primarily affected

by the impingement of slurry particles and corrosion. On the other hand, SEM morphology of the coated specimens' eroded surfaces exhibited that the material removal mechanism is greatly affected by erosion and abrasion [21]. Though corrosion is insignificant, it may be ascribed to the remarkable corrosion resistance of the coating. Besides, the coating substrate stays intact, with very few flakes, craters, and cracks after the slurry test, which are predominantly affected by the impinging particles, substantiating the abrasive wear mechanism.

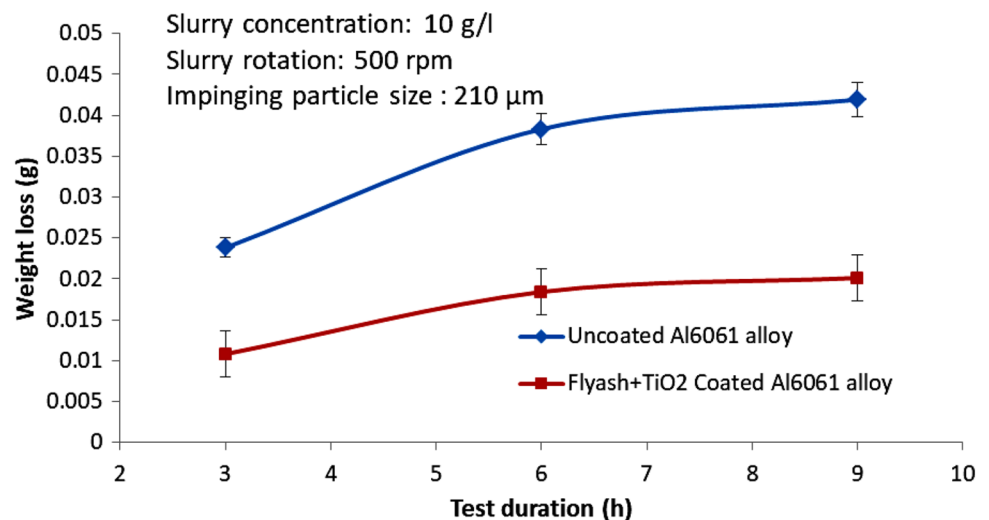
### 3.4.4 Influence of Test Duration

Figure 13 illustrates the weight loss variation during slurry erosion wear of both Al-6061 substrate and the synthesized composite coatings with different test durations of 3, 6, and 9 h at fixed impinging particle size, slurry speed, and concentration. It is seen that the magnitude of damage surges with amplified test durations for both uncoated and coated specimens. As the contact time between the erodent and target surface increases, the kinetic energy and the erodent particles' momentum are transferred to the target surface during the collision between particles leading to more excessive material removal [2, 11]. Exhaustive studies on worn surfaces after the slurry erosive test are shown in Fig. 14a–f that disclose the hard-hitting erosion on an uncoated substrate compared to specimens with Flyash-TiO<sub>2</sub>-coated substrate. The observation of plastically deformed craters results from sand particles' abrasive action forming cracks due to micro-cutting, which influences the material removal and the lower relative hardness substrate than the corrosion on uncoated Al-6061. The non-interrupted mechanical movement of sand particles results in contact of slurry with fresh areas of the specimen. Consequently, the localized corrosion rate increases due to formation of corrosion pits and salt attack on the sample. Thus, the increased material removal



**Fig. 12** a–f SEM of eroded surfaces at different impinging particle size. **a** and **b** Uncoated and coated substrate at 210  $\mu\text{m}$ . **c** and **d** Uncoated and coated substrate at 300  $\mu\text{m}$ . **e** and **f** Uncoated and coated substrate at 425  $\mu\text{m}$

**Fig. 13** Weight loss at different test durations



rate is caused by the combination of corrosive and erosive action [4, 8, 21].

On the surface of the coated samples, there is no indication of the presence of corrosion pits. Corrosion generally relates to electrolyte ions' penetration to the base materials through defects or porous within the coatings. The magnitude of penetration relies upon the sum of such flaws. Therefore, the improved erosion-corrosion resistance and most minor damage of coatings surfaces are in turn relayed on the minimal micro-level defects as witnessed in the SEM images.

Few ploughing and impinging marks are seen on the surfaces of coated specimens representing brittle rupture. The material has been removed on the coated surface by frequent abrasive and impact action of solid particles resulting in small splat ejection. It can be concluded that the increased test duration would enhance the harshness of erosion-corrosion, and the impinging of silica sand becomes a significant factor leading to increased deterioration of the surface [2, 13, 24–26]. It is observed that under all the studied test durations, Flyash-TiO<sub>2</sub>-coated Al-6061 substrate possesses superior slurry wear resistance when compared with uncoated Al-6061 alloy.

The CM was used to examine the morphology of eroded surfaces of uncoated and coated substrates under varying test durations. The 3D-eroded surface topography was observed over 1280 × 1280  $\mu\text{m}$  and illustrated in Fig. 15a–f. The deteriorated surface contour of all the coated specimens was the almost uniform and flat surface morphology. Uncoated eroded substrate topography shows the wide-ranging surface undulations united with the large and deep craters, in line with the SEM observations. The negligible surface deterioration of the developed Flyash-TiO<sub>2</sub> composite coatings on

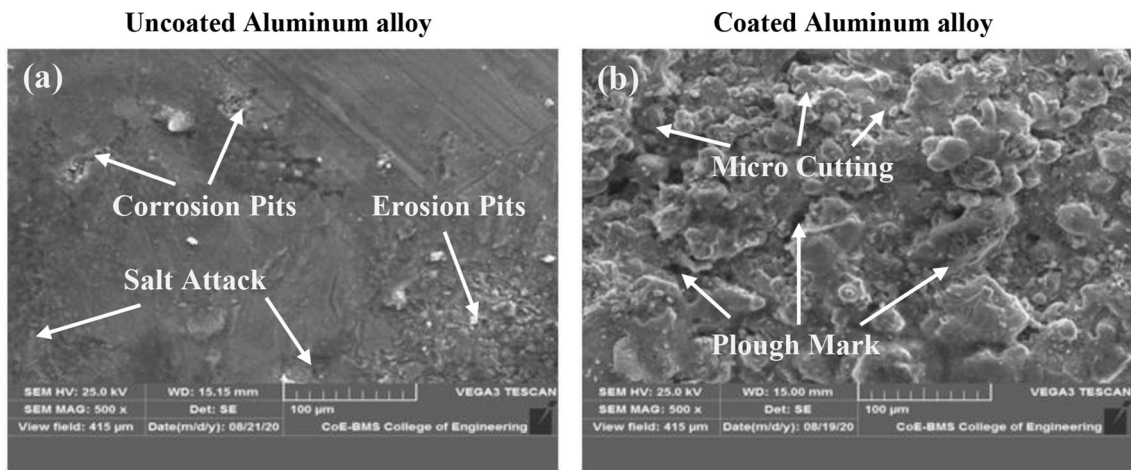
the Al-6061 substrate advocates superior erosion resistance compared to the uncoated Al-6061.

### 3.5 Effect of Coating for Slurry Erosive Wear

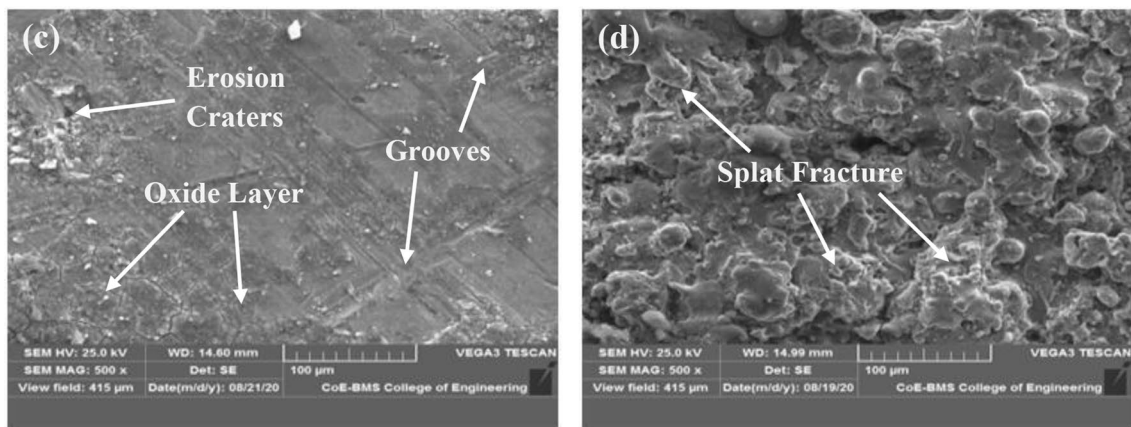
The weight loss of uncoated and coated Al-6061 substrate tested under the slurry concentrations of 10 g/l, slurry revolving speed 500 rpm, impinging particle sizes 210  $\mu\text{m}$ , and 9 h test duration are presented in Fig. 16. It is seen that the weight loss for Flyash-TiO<sub>2</sub>-coated Al-6061 substrate is significantly lower when evaluated with the uncoated sample. The developed coatings offer a maximum of 52% enhancement in slurry wear resistance when compared with uncoated Al-6061 substrate. A rise in the slurry erosive resistance of the coated sample is primarily due to improved coating materials' hardness. The hard Titania and Flyash composite coatings impose enhanced resistance to the impinging particles and lower the material loss, as discussed.

Overall, the slurry erosive wear performances of the developed composite coatings are remarkably better than the uncoated aluminum alloy under all the slurry test conditions studied. However, the limitation of the present work includes the fact that the coating performance is evaluated under uncontrolled flow conditions. Evaluation of slurry erosive wear under controlled flow conditions would be interesting to explore. Further, the corrosion performance of the composite coatings may be evaluated by the electrochemical method to understand the corrosion mechanism and contribution. It is also fascinating to assess the erosion performance coatings at elevated temperatures under acidic conditions considering the application of the developed coatings in the chemical industries.

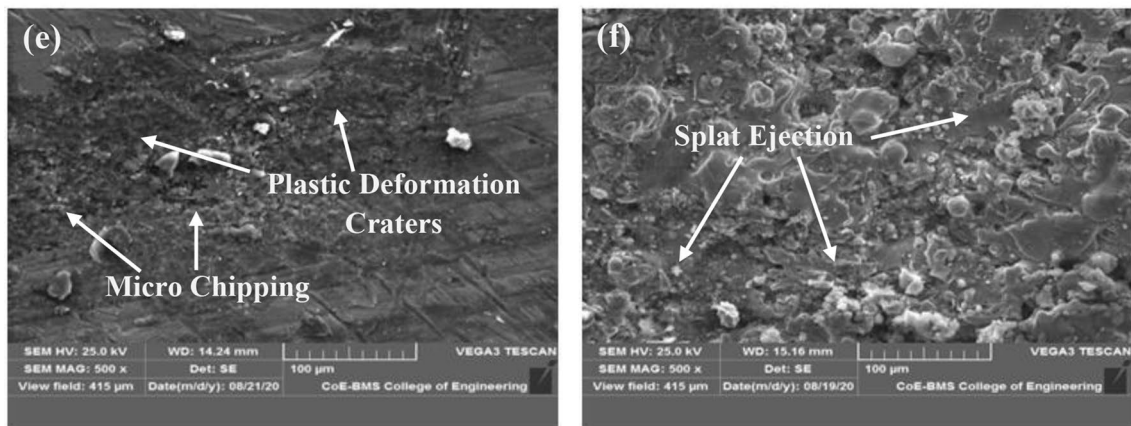




(a) & (b) uncoated and coated substrate at 3 hours



(c) & (d) uncoated and coated substrate at 6 hours



(e) & (f) uncoated and coated substrate at 9 hours

**Fig. 14** a–f SEM of eroded surfaces at different test durations. a and b Uncoated and coated substrate at 3 h. c and d Uncoated and coated substrate at 6 h. e and f Uncoated and coated substrate at 9 h

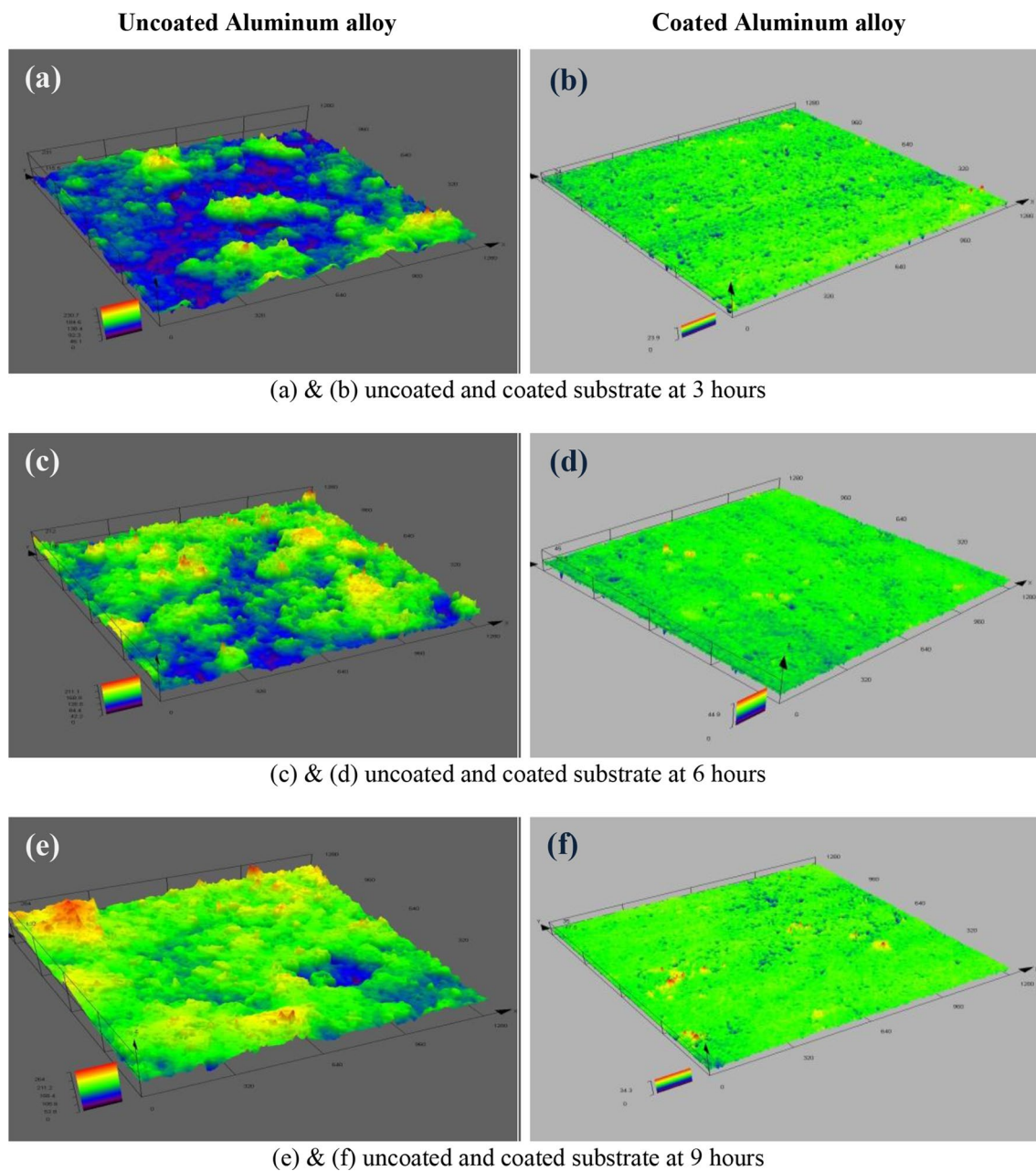


**Fig. 15** a–f Confocal micrograph images of eroded surfaces at different test durations. **a** and **b** Uncoated and coated substrate at 3 h. **c** and **d** Uncoated and coated substrate at 6 h. **e** and **f** Uncoated and coated substrate at 9 h

## 4 Conclusions

- Composite coatings of Flyash-TiO<sub>2</sub> were deposited on the substrate of Al-6061 alloy by plasma spray technique under optimum process parameters. Microstructural analysis of synthesized coatings confirms homogeneous and intense deposition of splats without any visible cracks or defects.
- A remarkable enhancement in micro-hardness is recorded in Flyash-TiO<sub>2</sub> coatings (454 HV<sub>5N</sub>) compared with uncoated Al-6061 substrate (70 HV<sub>5N</sub>).
- Slurry wear performance of uncoated and coated specimens under varied test conditions was investigated. It was observed that the coated samples exhibited a maximum of 52% enhancement in slurry erosive wear resistance than the uncoated Al-6061 alloy.

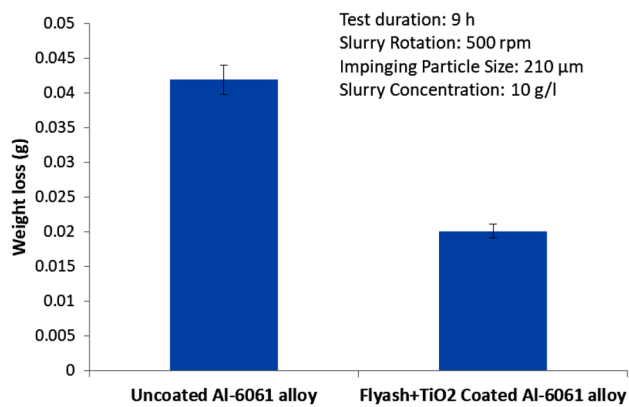


**Fig. 16** Slurry erosive wear loss variation for uncoated and coated Al-6061

- The magnitude of damage surges with amplified test conditions for both uncoated and coated specimens. The micrographs of worn surfaces unveiled the severe erosion marks on uncoated substrates. Multiple indentation pits, grooves, craters, and corrosion pits have been observed on eroded surfaces of uncoated specimens due to poor surface hardness and corrosion resistance than the coated substrate.
- The coated surfaces remain intact after the slurry test, with very few brittle, macro-, and micro-splat fractures and impinging marks substantiating the erosion and abrasive wear mechanism. This experimental study's notable feature is that the coated specimens have dominantly endured under the severe erosion conditions compared to the uncoated substrate.
- The 3D surface topography was analyzed using confocal microscopy. The eroded surfaces of uncoated specimens show the wide-range surface undulations united with the large and deep craters than the coated samples. This confirms the superior erosion resistance of Flyash-TiO<sub>2</sub> composite coatings under all the studied test conditions.

**Acknowledgements** The authors wish to acknowledge their sincere thanks to Vision Group of Science and Technology (VGST), Government of Karnataka, INDIA, for sponsoring this research work (Project No.: KSTePS/VGST/RGS/F/2017-18/GRD-718/41/2018-19/204).

## References

1. Yang K, Rong J, Liu C, Zhao H, Tao S, Ding C (2016) Study on erosion-wear behavior and mechanism of plasma-sprayed alumina-based coatings by a novel slurry injection method. *Tribol Int*. <https://doi.org/10.1016/j.triboint.2015.09.007>
2. Naveena BE, Keshavamurthy R, Sekhar N (2017) Slurry erosive wear behaviour of plasma-sprayed flyash-Al<sub>2</sub>O<sub>3</sub> coatings. *Surf Eng*. <https://doi.org/10.1080/02670844.2017.1288341>
3. Naveena BE, Keshavamurthy R, Sekhar N (2019) Comparative study on effects of slurry erosive parameters on plasma sprayed flyash- Al<sub>2</sub>O<sub>3</sub> and flyash-SiC composite coatings on Al-6061 alloy. *Int J Comput Mater Sci Surf Eng* 8(1):57–75
4. Keshavamurthy R, Naveena BE, Sekhar N (2018) Thermal spray coatings for erosion-corrosion protection. IGI Global, Hershey. <https://doi.org/10.4018/978-1-5225-4194-3.ch010>
5. Fauchais PL, Heberlein JV, Boulos MI (2014) Thermal spray fundamentals, from powder to part. Springer, New York. [https://doi.org/10.1007/978-0-387-68991-3\\_2](https://doi.org/10.1007/978-0-387-68991-3_2)
6. Fauchais P, Vardelle A (2012) Thermal sprayed coatings used against corrosion and corrosive wear. In: Jazi H (ed) *Advanced plasma spray applications*. IntechOpen, London
7. Naveena BE, Keshavamurthy R, Sekhar N (2018) "Dry sliding wear behaviour of plasma sprayed flyash-Al<sub>2</sub>O<sub>3</sub> and Flyash-SiC coatings on the Al-6061 aluminum alloy. *SILICON*. <https://doi.org/10.1007/s12633-018-9978-x>
8. Sathiyamoorthy R, Shanmugam K, Balasubramanian V (2017) Erosive wear behavior of SiC reinforced Titania coating deposited by high velocity oxy (HVOF) fuel spraying. *Adv Nat Appl Sci* 11(8):9–14
9. Reyes Mojena MA, Sánchez Orozco M, CarvajalFals H, Sagaró Zamora R, Camello Lima CR (2017) A comparative study on slurry erosion behavior of HVOF sprayed coatings. *DYNA* 84(202):239–246
10. Heimann RB, Lehmann HD (2008) Recently patented work on thermally sprayed coatings for protection against wear and corrosion of engineered structures. *Recent Pat Mater Sci* 1:41–55
11. Zhao HX, Goto H, Matsumura M, Takahashi T, Yamamoto M (1999) Slurry erosion of plasma-sprayed ceramic coatings. *Surf Coat Technol* 115:123–131
12. Ramesh CS, Kumar RS, Murthy M, Harsha (2014) Slurry erosive wear behaviour of copper plasma sprayed with Titania-30wt% inconel 718. *Proced Mater Sci* 5:1130–1135
13. Chinnakurli Suryanarayana R, Rupanagudi SK, Nagaraj A (2016) Slurry erosive wear behaviour of TiO<sub>2</sub>-30 wt% inconel-718 plasma sprayed coatings on Al-6061 substrate. The Society of Tribologists and Lubrication Engineers (STLE), Park Ridge
14. Ahmad Z, Khan AU, Farooq R, Saif T, Mastoi NR (2016) Mechanism of corrosion and erosion resistance of plasma-sprayed nano-structured coatings. Intech Open, London
15. Matikainen V, Niemi K, Koivuluoto H, Vuoristo P (2014) Abrasion, erosion and cavitation erosion wear properties of thermally sprayed alumina based coatings. *Coatings* 4:18–36. <https://doi.org/10.3390/coatings4010018>
16. Keshavamurthy R, Naveena BE, Ahamed A, Sekhar N, Peer D (2019) Corrosion characteristics of plasma sprayed flyash-SiC and Flyash-Al<sub>2</sub>O<sub>3</sub> composite coatings on the Al-6061 alloy. *Mater Res Express*. <https://doi.org/10.1088/2053-1591/ab28e1>
17. Sahu SP, Satapathy A, Patnaik A, Sreekumar KP, Ananthapadmanabhan PV (2010) Development, characterization and erosion wear response of plasma sprayed fly ash-Al coatings. *Mater Des* 31:1165–1173
18. Mishra SC, Mishra PC, Rout KC, Ananthapadmanabhan PV (1999) Fly ash as a coating material for plasma spray coatings. *Proceedings of the national seminar on fly ash utilisation*. NML, Jamshedpur, pp 131–135
19. Sidhu BS, Singh H, Puri D, Prakash S (2007) Wear and oxidation behaviour of shrouded plasma sprayed fly ash coatings. *Tribol Int* 40:800–808
20. Yılmaz Ş, Okumuş SC, Demirkıran AŞ, Bindal C (2004) Fly ash based plasma spray coating. *Key Eng Mater* 264–268:533–536
21. Ramesh CS, Sekhar N, Keshavamurthy R, Pramod S (2007) A study on slurry erosion and corrosion behaviour of HVOF sprayed titania coatings. *Int J Surf Sci Eng*. <https://doi.org/10.1504/IJSURFSE.2015.067039>

22. Singh VP, Sil A, Jayaganthan R (2014) Evaluation of dry sliding and slurry erosion behaviour of plasma sprayed nanostructured  $\text{Cr}_2\text{O}_3$ - $3\text{TiO}_2$  coatings, tribology—materials. *Surf Interfaces* 8(3):131–138. <https://doi.org/10.1179/1751584X13Y.0000000054>
23. Grewal HS, Arora HS, Agrawal A, Singh H, Mukherjee S (2013) Slurry erosion of thermal spray coatings: effect of sand concentration. *Proced Eng* 68:484–490
24. Joshi AG, Kumar MP, Basavarajappa S (2014) Influence of  $\text{Al}_2\text{O}_3$  filler on slurry erosion behavior of glass/epoxy composites. *Proced Mater Sci* 5:863–872
25. Ramachandran CS, Balasubramanian V, Ananthapadmanabhan PV (2013) Erosion of atmospheric plasma sprayed rare earth oxide coatings under air suspended corundum particles. *Ceram Int* 39(1):649–672
26. Algahtani A, Neville A, Shrestha S (2013) Tomasz liskiewicz “erosion resistance of surface engineered 6000 series aluminium alloy.” *J Eng Tribol* 227(11):1204–1214

**Publisher's Note** Springer Nature remains neutral with regard to jurisdictional claims in published maps and institutional affiliations.